Quantum Computing Quantum Monte Carlo

Yukun Zhang,[1,2,*] Yifei Huang,[3,*] Jinzhao Sun,[4,5] Dingshun Lv,[3] and Xiao Yuan[1,2,†]

[1] *Center on Frontiers of Computing Studies, Peking University, Beijing 100871, China*
[2] *School of Computer Science, Peking University, Beijing 100871, China*
[3] *ByteDance Ltd., Zhonghang Plaza, No. 43, North 3rd Ring West Road, Haidian District, Beijing, China*
[4] *Clarendon Laboratory, University of Oxford, Parks Road, Oxford OX1 3PU, United Kingdom*
[5] *Quantum Advantage Research, Beijing 100080, China*

Quantum computing and quantum Monte Carlo (QMC) are respectively the most powerful quantum and classical computing methods for understanding many-body quantum systems. Here, we propose a hybrid quantum-classical algorithm that integrates these two methods, inheriting their distinct features in efficient representation and manipulation of quantum states and overcoming their limitations. We introduce upper bounds to non-stoquaticity indicators (NSI), which measure the sign problem, the most notable limitation of QMC. We show that our algorithm could greatly mitigate the sign problem, which decreases NSIs with the assist of quantum computing. Meanwhile, the use of quantum Monte Carlo also increases the power of noisy quantum circuits, allowing accurate computation with much shallower circuits. We numerically test and verify the method for the N_2 molecule (12 qubits) and the Hubbard model (16 qubits). Our work paves the way to solving practical problems with intermediate-scale and early-fault tolerant quantum computers, with potential applications in chemistry, condensed matter physics, materials, high energy physics, etc.

A critical task in quantum physics is to find ground (excited) eigenstates and eigenenergies of a quantum many-body system with wide applications in quantum chemistry [1–3], materials [4], condensed matter physics [5], high energy physics [6, 7], etc. Based on different assumptions or approximations, various classical computational methods have been invented, such as perturbation theories [8], variational tensor network approaches [9–11], self-consistent density functional theory or embedding methods [12–16], quantum Monte Carlo (QMC) [17–19], machine learning [20–22], etc. In particular, as one of the state-of-the-art approaches, QMC has drawn great attention and been widely exploited to study chemistry and condensed matter physics problems, solving problems with up to around 800 electrons [23]. However, since the Hilbert space of quantum systems increases exponentially with the system size, all these classical methods have certain limitations. Specifically, QMC represents quantum states by an effective superposition of classical basis states, which is realized via a sampling approach, it in general suffers from the notorious sign problem, prohibiting its usefulness for general problems.

On the other hand, quantum computers can more naturally represent and manipulate quantum states, thus offering the opportunity to overcome the challenge [24]. Different quantum algorithms, such as adiabatic state preparation [25], quantum phase estimation [26–28], and the recent proposed/improved methods [29–33], have been proposed to solve the eigenstate problem. Yet, those quantum algorithms generally require a deep quantum circuit that is only achievable with a fault-tolerant universal quantum computers. Near-term quantum computers however can only control a limited number of qubits with relatively noisy operations, corresponding to the noisy intermediate-scale quantum (NISQ) era. While many recent works have shown the potential applicability of quantum computing using NISQ devices [34–38], whether they are sufficiently powerful (large and accurate) to solve realistic problems still remains open.

Here we introduce a hybrid approach that integrates quantum Monte Carlo and quantum computing, leveraging their complementary strengths in representing and processing quantum states, meanwhile mitigating their respective weaknesses of exponentially small average signs and hardware limitations. We first introduce upper bounds of the non-stoquaticity indicator (NSI), which measures the seriousness of the sign problem. Then we consider full configuration interaction quantum Monte Carlo (FCIQMC) [19, 39], and show how to efficiently implement it using a quantum computer. Since the quantum states (walkers) are now prepared with an optimized quantum circuit, the sign problem of FCIQMC is greatly relieved. This has been verified numerically for the N_2 molecule (12 qubits) and the Hubbard model (16 qubits). We show a drastic decrease of the NSI, the energy variance (with fixed number of walkers), and the number of walkers (to ensure a desired variance) using our method. The results also show much higher accuracies for QC-FCIQMC, which are only achievable with much deeper circuits for conventional quantum computing approaches.

Background. — Here we review the basics of QMC and quantum computing. We consider the problem of finding the ground state of Hamiltonian H. We focus on H with real matrix elements and refer to Supplementary Materials for the general case.

We focus on projector QMC, a subclass of QMC, which effectively represents the state as a superposition of walkers (states such as Slater determinants) and realizes the imaginary-time evolution (ITE) of the state by stochastically propagating the walkers. Denote the walkers by

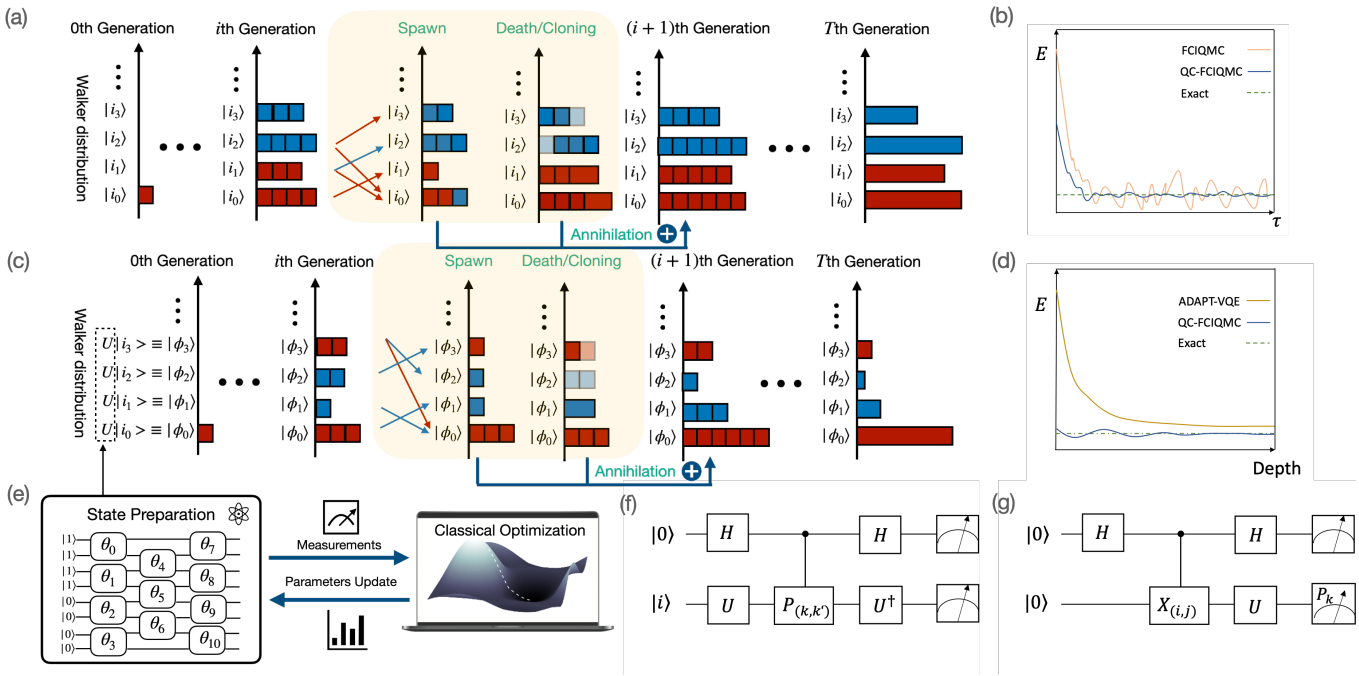

Figure 1. (a) Sketch of the spawning, death/cloning and annihilation steps in FCIQMC. Red and blue colors represent walkers with positive and negative signs respectively. Red and blue arrows represent the sign of H_{ji}. The transparent boxes represents dead walkers, while the elongated walkers are the cloned ones. (b) Sign problem comparison for our QC-FCIQMC and FCIQMC. (c) Procedure of QC-FCIQMC. The quantum circuit U that generates the new basis are obtained from VQAs, such as the one shown in (e). (d) Energy convergence comparison of ADAPT-VQE and QC-FCIQMC. (f) Quantum circuits for evaluating $|H_{ji}|^2$. (g) Circuit for evaluating the real part of H_{ji}.

$\{|i\rangle\}$ and the initial state by $|\psi(0)\rangle = \sum_i c_i(0)\,|i\rangle$ with coefficients $c_i(0)$, projector QMC aim to realize the ITE of the state as $|\psi(\tau)\rangle \propto e^{-(H-S)\tau}\,|\psi(0)\rangle$ with time $\tau > 0$ and certain parameter S. Specifically, for FCIQMC (see Fig. 1(a)), we first generate $N_i(\tau)$ number of the walker $|i\rangle$ at time $\tau = 0$; Then, for small time $\Delta\tau$, we repeatedly update each walker $|i\rangle$ through (1) spawning — spawn a child walker $|j\rangle$ ($j \neq i$) with probability $|H_{ji}|\Delta\tau$ with the same sign as walker $|i\rangle$ multiplied by the sign of $H_{ji}/|H_{ji}|$ ($H_{ij} = \langle i|H|j\rangle$); (2) Death or cloning — the walker $|\phi_i\rangle$ dies with probability $(H_{ii} - S)\Delta\tau$ (if $H_{ii} - S > 0$) and clones itself with probability $|(H_{ii} - S)|\Delta\tau$ otherwise; (3) Annihilation — annihilate same walker pairs with opposite signs. While QMC could deterministically find the ground state with large τ, it suffers from the sign problem. Specifically, since the walkers may have both positive and negative signs, the average sign generally decreases exponentially with time τ and the system size. We will show a quantitative measure of the sign problem shortly.

For quantum computing, we focus on variational quantum algorithms (VQA) designed for near-term quantum devices (see Fig. 1(e)). Here, we consider variational quantum eigensolver (VQE) [40, 41] as an example. For the Hamiltonian H, we approximate its ground state as $|\phi(\vec{\theta})\rangle = U(\vec{\theta})\,|\bar{0}\rangle$ with a parameterized quantum circuit $U(\vec{\theta})$ and an initial state $|\bar{0}\rangle$. Then we apply a classical optimizer to search for parameters $\vec{\theta}$ that minimize the energy $E(\vec{\theta}) = \langle\phi(\vec{\theta})|H|\phi(\vec{\theta})\rangle$. Since quantum computers could more efficiently represent and process quantum states, recent works have demonstrated the potential power of variational quantum algorithms [34–38]. Yet, they also have several limitations. First, due to short coherence time of near-term quantum devices, the circuit depth is limited, which may be incapable to approximate the desired ground state [42, 43]. Meanwhile, noise in quantum gates is also detrimental to the computation accuracy, making it hard to surpass classical methods [44–47]. At last, the landscape of $E(\vec{\theta})$ with deep circuits might have barren plateau or many local minima, and thus its optimization could also be challenging [48–50].

Shortly, we introduce our hybrid approach that could overcome or mitigate these limitations of QMC and VQAs, see Fig. 1(b, d).

Sign problem indicators.— According to Troyer [51], a necessary condition for the sign problem is non-stoquasticity. Specifically, the Hamiltonian is called "stoquastic" when all its off-diagonal terms (in the walker basis) are non-positive. In the following, we consider a general walker basis (orthonormal states) $\{|\phi_i\rangle\}$. For a thermal state $e^{-\beta H}/Z$ with $Z = \mathrm{Tr}[e^{-\beta H}]$, the expectation of observable A is $\langle A\rangle = \mathrm{Tr}[Ae^{-\beta H}]/Z$. Denote

$G = \alpha I - H$ with $\alpha = \max_i H_{ii}$, and we have

$$\langle A\rangle = \frac{\mathrm{Tr}[Ae^{\beta G}]}{\mathrm{Tr}[e^{\beta G}]} = \frac{\sum_{k=0}^{\infty}\frac{\beta^k}{k!}\sum_{i_0,i_1,\ldots i_k} A_{i_0 i_1}G_{i_1 i_2}\cdots G_{i_k i_0}}{\sum_{k=0}^{\infty}\frac{\beta^k}{k!}\sum_{i_1,i_2\ldots i_k} G_{i_1 i_2}G_{i_2 i_3}\cdots G_{i_k i_1}}, \tag{1}$$

where we denote $M_{ij} := \langle\phi_i|M|\phi_j\rangle$ for any operator M. When H is stoquastic, every element of G is positive, and so is the expanded terms of $\mathrm{Tr}[e^{\beta G}]$. On the other hand, when H_{ij} has positive off-diagonal terms, the expansion has a mixture of signs, leading to the sign problem.

To quantify the sign problem of Hamiltonian H, we separate it by $H = H_+ + H_-$ with nonzero elements $(H_-)_{ij} = H_{ij}$ ($[i = j]$ *or* $[i \neq j$ *and* $H_{ij} < 0]$) and $(H_+)_{ij} = H_{ij}$ $[i \neq j$ *and* $H_{ij} > 0]$. The bosonic form [51] of H is $\tilde{H} = H_- - H_+$, which is stoquastic and hence has no sign problem. The non-stoquasticity indicator (NSI) is defined by

$$S(H) = \frac{\mathrm{Tr}[e^{-\beta\tilde{H}}] - \mathrm{Tr}[e^{-\beta H}]}{\mathrm{Tr}[e^{-\beta H}]}. \tag{2}$$

Denote s to be the sign of the expansion of $\mathrm{Tr}[e^{\beta G}]$ in Eq. (1), then we have $S(H) = 1/\langle s\rangle - 1$. The sign problem indicates an exponentially small average sign $\langle s\rangle = e^{-\beta\Delta f}$ with Δf being the free energy difference between H and $\tilde{H}$. Thus $S(H)$ also exponentially increases with $\beta\Delta f$. However, it is in general hard to evaluate Δf. Here, we provide an upper bound of $S(H)$ with more explicit dependence on the matrix element of the Hamiltonian $H_\pm$.

Theorem 1. *The non-stoquasticity indicator is upper bounded by*

$$S(H) \leq 2e^{\beta\|(\alpha - H_-)\|_{L_1}}\sinh(\beta\|H_+\|_{L_1}), \tag{3}$$

where we define the matrix norm as $\|M\|_{L_1} := \sum_{i,j}|M_{ij}|$ *for matrix* M.

A stoquastic Hamiltonian has $H_+ = 0$, which indicates $S(H) = 0$ and hence no sign problem. In general, a smaller $\|H_+\|_{L_1}$ also corresponds to a less serious sign problem, which is consistent with recent works [52–55].

Meanwhile, when we focus on the imaginary time evolution of a specific initial state, say ϕ_0, with time $\tau = \beta/2$, we can similarly define the NSI as

$$S(H,\phi_0) = \frac{\langle\phi_0|e^{-\beta\tilde{H}}|\phi_0\rangle - \langle\phi_0|e^{-\beta H}|\phi_0\rangle}{\langle\phi_0|e^{-\beta H}|\phi_0\rangle}. \tag{4}$$

Again, $S(H,\phi_0)$ measures the sign problem and is related to the average sign. We provide an upper bound of $S(H,\phi_0)$ as a function of ϕ_0 and $H_\pm$.

Theorem 2. *The non-stoquasticity indicator is upper bounded by*

$$S(H,\psi_0) = \mathcal{O}\left(\|\Pi_\perp H|\phi_0\rangle\|^2\right), \tag{5}$$

where $\||v\rangle\| = \sqrt{\langle v|v\rangle}$ *and* $\Pi_\perp = I - |\phi_0\rangle\langle\phi_0|$.

Here, we have ignored the dependence on other matrix elements of H and we refer to Supplementary Materials for the complete upper bound. We can see that apart from small H_+, a good initial state that is close to an eigenstate of H can also alleviate the sign problem. Note that the upper bounds of Theorem 1 and 2 are not tight, and the NSI could be much smaller in reality.

QC-FCIQMC.— We now introduce our hybrid algorithm using a quantum computer to mitigate the sign problem of QMC. The basic idea is to replace the simple walker states $\{|i\rangle\}$ with states $\{|\phi_i\rangle\}$ prepared by quantum circuits $|\phi_i\rangle = U|i\rangle$, as shown in Fig. 1(c). This is equivalent to consider walkers $\{|i\rangle\}$ with a similarity transformed Hamiltonian $U^\dagger HU$. We may use a quantum computer to find U that approximately diagonalizes H [56, 57], where the off-diagonal part $U^\dagger HU$ is suppressed. One may argue that why we need QMC if we could already diagonalize H. The motivation is that exactly diagonalizing H might need a deep quantum circuit, which is beyond the capability of near-term quantum devices. Contrarily, we only need to approximately diagonalize H with a shallow circuit and apply QMC to further improve the accuracy. Furthermore, according to Theorem 2, we may not even need to diagonalize H, but just find an approximate eigenstate, which is a much simpler task and requires even shallower circuits [41, 58–61]. We can apply VQAs such as VQE with an even shorter circuit, but still run QMC with eased sign problems (see Fig. 1(b)). Meanwhile, the algorithm also improves the power of quantum computing with NISQ hardware (see Fig. 1(d)).

Suppose we already find the unitary U using either approximate Hamiltonian diagonalization [56, 57] or VQE [41, 58–61], and replace $|i\rangle$ with $|\phi_i\rangle = U|i\rangle$, the wavefunction is expanded as $|\psi(\tau)\rangle = \sum_i c_i(\tau)|\phi_i\rangle$ and the coefficients $c_i(\tau)$ follow the imaginary time evolution as

$$\frac{\mathrm{d}c_i(\tau)}{\mathrm{d}\tau} = -\sum_j (H_{ij} - S\delta_{ij})c_j(\tau), \tag{6}$$

with $H_{ij} = \langle\phi_i|H|\phi_j\rangle$ and an adjustable energy shift S. Now, we need to propagate the (quantum) walkers to effectively realize the imaginary time evolution. Here, a major challenge is how to realize the spawning process, i.e., to propagate walker $|\phi_i\rangle$ to $|\phi_j\rangle$ with probability $|H_{ji}|\Delta\tau$. In conventional FCIQMC, this is possible since there is only a polynomial number of nonzero H_{ji} for (classical) walkers $\{|i\rangle\}$. However, for (quantum) walkers $|\phi_i\rangle$, there might be an exponential number of nonzero H_{ji}, so naively, we may need to measure all H_{ji} to realize the spawning process, which is formidable.

Here we introduce an efficient way to realize the spawning process. To evaluate the probability $|H_{ji}|\Delta\tau$, we note that $|H_{ji}|^2 = \langle i|U^\dagger HU\Pi_j U^\dagger HU|i\rangle$ with $\Pi_j = |j\rangle\langle j|$. Suppose the Hamiltonian is expanded as

$H = \sum_k h_k P_k$ with coefficients h_k and Pauli operators P_k, then $|H_{ji}|^2 = \sum_{kk'} h_k h_{k'} p^i_{kk'}(j)$ with probability $p^i_{kk'}(j) = \langle i|U^\dagger P_k U \Pi_j U^\dagger P_{k'} U|i\rangle$ satisfying $p^i_{kk'}(j) \geq 0$ and $\sum_j p^i_{kk'}(j) = 1$. For fixed i, k, k', we can use the quantum circuit in Fig. 1(f) to measure $p^i_{kk'}(j)$ for all j and hence obtain $|H_{ji}|$ up to a desired accuracy. We ususally get a small number of nonzero $|H_{ji}|$. Then we can apply the quantum circuit in Fig. 1(g) to further estimate the sign (phase) of H_{ji}. Note that the quantum circuits for estimating $|H_{ji}|$ and its sign only introduce one ancillary qubit and at most doubles the unitary U (apart from few gates independent of U). Meanwhile, H_{ji} only needs to be measured once and information could be re-used.

We can also efficiently estimate each H_{ii} using the same quantum circuit and hence realize the death or cloning step. The last annihilation step does not need the quantum computer. After implementing the evolution (with initial walkers ϕ_0), we can get the the energy by the mixed energy evaluation $E(\tau) = E_0 + \sum_{i\neq 0} \langle\phi_i| H |\phi_0\rangle \frac{\text{sign}(i) N_i(\tau)}{N_0(\tau)}$, where $E_0 = \langle\phi_0|H|\phi_0\rangle$, and $N_i(\tau)$ and $\text{sign}(i)$ are the number and sign of walker ϕ_i, respectively, at time τ. Suppose ϕ_0 is obtained by running VQE, then our method effectively introduces corrections from all other ϕ_i by implementing QMC. We summarize the workflow in Fig. 1(c) and Algorithm 1. We used VQE in the algorithm as an example, but it works for general VQAs.

Algorithm 1 QC-FCIQMC

Input: Hamiltonian H, total evolution time T, time step $\Delta\tau$.
Output: Ground state energy estimation.

```
Run VQE to determine U and hence {|φ_i⟩ = U|i⟩}.
Generate N_0 walkers |φ_0⟩ and let walker set D = {0}.
for n in range(T/Δτ) do
    for i in D do
        Estimate |H_ji| using the circuits in Fig. 1(f) [62].
        for j with nonzero |H_ji| do          ▷ Spawning step
            For each walker |φ_i⟩, spawn a new walker |φ_j⟩ with
            probability Δτ|H_ji|.
            if New walker |φ_j⟩ spawned then
                Estimate H_ji/|H_ji| using the circuit in Fig. 1(g)
                Label the new walker |φ_j⟩ with the sign of |φ_i⟩
                multiplied by the sign H_ji/|H_ji|.
                Add j to D.
        Estimate p_i = Δτ(H_ii − S)
        if p_i < 0 then                       ▷ Death/cloning step
            Clone each walker |φ_i⟩ with probability |p_i|.
        else
            Kill each walker |φ_i⟩ with probability p_i.
        for i in S do                         ▷ Annihilation step
            Annihilate the walkers |φ_i⟩ with opposite signs.
Output the mixed energy.
```

Numerics.— Now we present numerical tests of the method. We consider two strongly correlated systems, the N_2 molecule and the Hubbard model. We compare our methods (QC-FCIQMC) to ADAPT-VQE [41, 58–61] and FCIQMC with single determinant walkers.

We first plot the potential energy surface of N_2 with different methods in Fig. 2(a). We freeze the 1s and 2s orbitals and run ADAPT-VQE with 12 qubits. The walker basis of our method is prepared by ADAPT-VQE circuits that add 12 fermionic operators. We set 10000 walkers to be the threshold for FCIQMC and our method to start the energy shift procedure. In Fig. 2(b), we plot the energy difference and standard deviation [63]. We see that QC-FCIQMC is able to push the results of shallow ADAPT-VQE circuits to the level of chemical accuracy across all bond lengths, much better than ADAPT-VQE and FCIQMC. Meanwhile, the standard deviation of QC-FCIQMC is much smaller than that of FCIQMC. Therefore, QC-FCIQMC would require a smaller evolution time and much fewer energy evaluations to obtain a precise energy estimation.

Next we consider how circuit depth (the number of operators added in ADAPT-VQE) affects our method. We focus on the N_2 molecule at bond length $4.0\mathring{A}$. Given a fixed 10000 number of walkers, we plot the effects of energy accuracy improvement and energy variance reduction with an increasing circuit depth in Fig. 2(c). The standard deviation is reduced by two orders from a single determinant basis (FCIQMC) to ADAPT-VQE with 24 operators (QC-FCIQMC). At this depth, QC-FCIQMC achieves the (pessimistically evaluated) standard deviation within the chemical accuracy using only 10000 walkers. Meanwhile, QC-FCIQMC also visibly outperforms ADAPT-VQE for all circuit depths. As shown in Fig. 2(d), the NSI upper bound also decreases with increasing circuit depths, verifying the theoretical result. In Supplementary Materials, we further show that the total number of walkers needed to ensure a fixed level of variance also decreases with the circuit depth.

We also test our QC-FCIQMC algorithm on the Hubbard model with $U/t = 4$, which exhibits competitions between onsite repulsion and hopping effects. In Fig. 2(e, f), we plot the energy fluctuations and walker distributions that manifest the sign problem for single determinant FCIQMC and QC-FCIQMC with 15 layers of Hamiltonian variational ansatz (HV ansatz) [64–66]. One can see that our QC-FCIQMC proposal significantly eases the influence of the sign problem. The fluctuation of the QC-FCIQMC energies is much smaller and the walker population is much more concentrated. We also test the systematic energy variance reduction with increasing number of HV ansatz layers, which can be found in the Supplementary Materials.

Discussion & Conclusion.— In this work, we propose a hybrid QC-QMC method. On the one hand, quantum computers is used to find a better walker basis, which alleviates the sign problem. On the other hand, QMC enhances the expressivity of shallow quantum circuits,

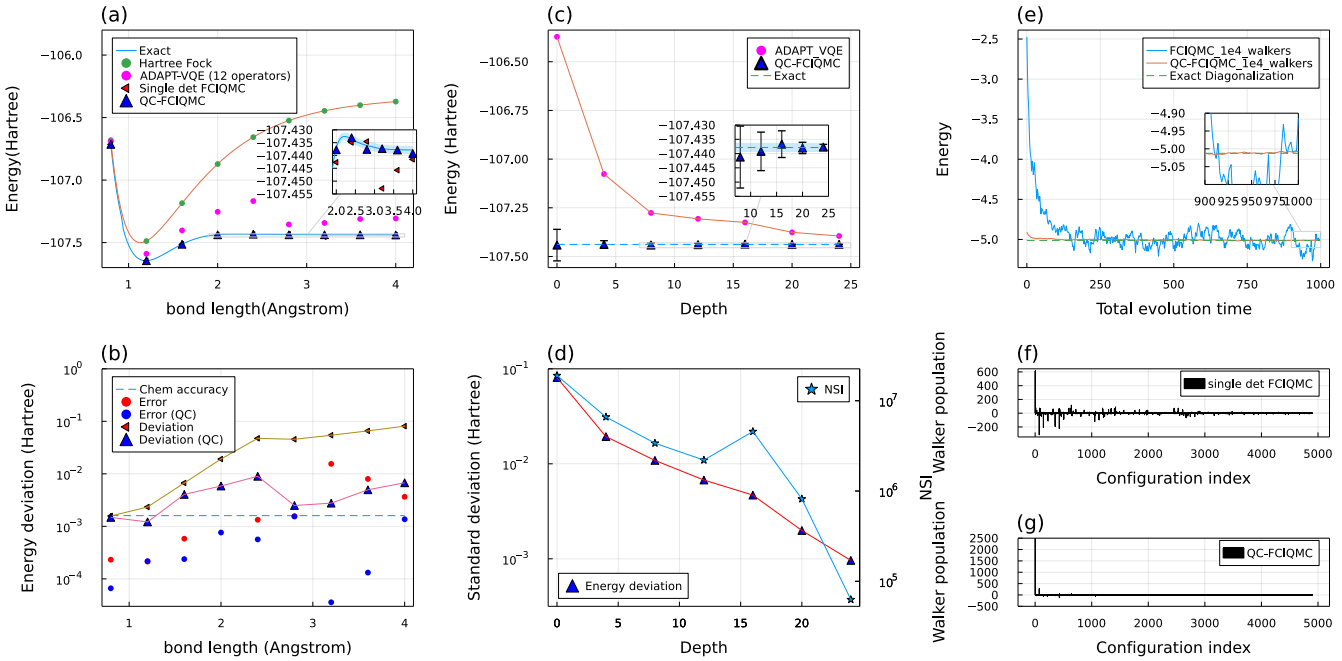

Figure 2. Numerical results of QC-FCIQMC. (a) Potential energy surface for the nitrogen molecule with different methods under the STO-3g basis set. (b) The standard deviation of energy evaluations along the QMC evolution. Here the new walker space of QC-FCIQMC are prepared with circuits from ADAPT-VQE (adding 12 fermionic operators for all bond length). (c) ADAPT-VQE energies and QC-FCIQMC energies with standard deviations for different depth of ADAPT-VQE. (d) Standard deviations from (c) as well as the non-stoquastic indicator with $\beta = 10^{-1}$. (e) Comparison of energy fluctuation for FCIQMC and QC-FCIQMC for the Hubbard model. (f) Walker population obtained from single determinant FCIQMC. (g) Walker population from QC-FCIQMC.

enabling more accurate computation with NISQ hardware. We derive upper bounds to NSIs, which guides the discovery and testing of the effectiveness of the method. The QC-FCIQMC algorithm also relies on a nontrivial efficient realization of the spawning process, which otherwise requires exponential resources. We benchmark the algorithm for N_2 and the Hubbard model, and the results show notable improvements over the single use of QC or FCIQMC.

There are several interesting future directions. First, the derived bounds for NSIs could be exploited to find basis rotation as a classical means to mitigate sign problems. Next, our algorithm is compatible with current and near-term quantum hardware, and therefore its detailed resource analysis, error mitigation, and experimental realization also deserve future works. Finally, we note that our method is distinct from recent other QC-QMC proposals [67–70], such as ones introducing quantum trial states in auxiliary field QMC. Yet, the comparison and combination of the ideas are interesting future directions.

ACKNOWLEDGEMENT

The authors thank Runze Chi, Tonghuan Jiang and Ji Chen for helpful discussion regarding the Hubbard model and QMC methods. This work is supported by the National Natural Science Foundation of China Grant No. 12175003.

* These authors contributed equally to this work.
† xiaoyuan@pku.edu.cn

[1] G. K.-L. Chan and S. Sharma, Annual review of physical chemistry **62**, 465 (2011).
[2] S. McArdle, S. Endo, A. Aspuru-Guzik, S. C. Benjamin, and X. Yuan, Reviews of Modern Physics **92**, 015003 (2020).
[3] Y. Cao, J. Romero, J. P. Olson, M. Degroote, P. D. Johnson, M. Kieferová, I. D. Kivlichan, T. Menke, B. Peropadre, N. P. Sawaya, *et al.*, Chemical reviews **119**, 10856 (2019).
[4] B. Bauer, S. Bravyi, M. Motta, and G. K.-L. Chan, Chemical Reviews **120**, 12685 (2020).
[5] B.-X. Zheng, C.-M. Chung, P. Corboz, G. Ehlers, M.-P. Qin, R. M. Noack, H. Shi, S. R. White, S. Zhang, and G. K.-L. Chan, Science **358**, 1155 (2017).
[6] S. P. Jordan, K. S. M. Lee, and J. Preskill, Science **336**, 1130 (2012).
[7] B. Nachman, D. Provasoli, W. A. de Jong, and C. W. Bauer, Phys. Rev. Lett. **126**, 062001 (2021).

[8] A. A. Abrikosov, L. P. Gorkov, and I. E. Dzyaloshinski, *Methods of quantum field theory in statistical physics* (Courier Corporation, 2012).

[9] A. Szabo and N. S. Ostlund, *Modern Quantum Chemistry: Introduction to Advanced Electronic Structure Theory* (Courier Corporation, 2012).

[10] R. Orús, Nature Reviews Physics **1**, 538 (2019).

[11] J. Jordan, R. Orús, G. Vidal, F. Verstraete, and J. I. Cirac, Physical review letters **101**, 250602 (2008).

[12] D. Sholl and J. A. Steckel, *Density Functional Theory: a Practical Introduction* (John Wiley & Sons, 2011).

[13] G. Knizia and G. K.-L. Chan, Physical review letters **109**, 186404 (2012).

[14] N. C. Rubin, arXiv preprint arXiv:1610.06910 (2016).

[15] W. Li, Z. Huang, C. Cao, Y. Huang, Z. Shuai, X. Sun, J. Sun, X. Yuan, and D. Lv, arXiv preprint arXiv:2109.08062 (2021).

[16] B. Bauer, D. Wecker, A. J. Millis, M. B. Hastings, and M. Troyer, Phys. Rev. X **6**, 031045 (2016).

[17] D. M. Ceperley and B. J. Alder, Physical review letters **45**, 566 (1980).

[18] S. Zhang, J. Carlson, and J. E. Gubernatis, Physical Review B **55**, 7464 (1997).

[19] G. H. Booth, A. J. Thom, and A. Alavi, The Journal of chemical physics **131**, 054106 (2009).

[20] G. Carleo and M. Troyer, Science **355**, 602 (2017).

[21] J. Hermann, Z. Schätzle, and F. Noé, Nature Chemistry **12**, 891 (2020).

[22] D. Pfau, J. S. Spencer, A. G. Matthews, and W. M. C. Foulkes, Physical Review Research **2**, 033429 (2020).

[23] Y. S. Al-Hamdani, P. R. Nagy, A. Zen, D. Barton, M. Kállay, J. G. Brandenburg, and A. Tkatchenko, Nature Communications **12**, 1 (2021).

[24] M. A. Nielsen and I. Chuang, *Quantum computation and quantum information* (American Association of Physics Teachers, 2002).

[25] T. Albash and D. A. Lidar, Reviews of Modern Physics **90**, 015002 (2018).

[26] A. Y. Kitaev, arXiv preprint quant-ph/9511026 (1995).

[27] D. S. Abrams and S. Lloyd, Physical Review Letters **83**, 5162 (1999).

[28] A. Aspuru-Guzik, A. D. Dutoi, P. J. Love, and M. Head-Gordon, Science **309**, 1704 (2005).

[29] L. Lin and Y. Tong, PRX Quantum **3**, 010318 (2022).

[30] K. Wan, M. Berta, and E. T. Campbell, arXiv preprint arXiv:2110.12071 (2021).

[31] P. Zeng, J. Sun, and X. Yuan, (2021), arXiv:2109.15304 [quant-ph].

[32] M. Huo and Y. Li, (2021), arXiv:2109.07807 [quant-ph].

[33] Y. Dong, L. Lin, and Y. Tong, (2022), arXiv:2204.05955 [quant-ph].

[34] J. Preskill, Quantum **2**, 79 (2018).

[35] E. Altman, K. R. Brown, G. Carleo, L. D. Carr, E. Demler, C. Chin, B. DeMarco, S. E. Economou, M. A. Eriksson, K.-M. C. Fu, M. Greiner, K. R. Hazzard, R. G. Hulet, A. J. Kollár, B. L. Lev, M. D. Lukin, R. Ma, X. Mi, S. Misra, C. Monroe, K. Murch, Z. Nazario, K.-K. Ni, A. C. Potter, P. Roushan, M. Saffman, M. Schleier-Smith, I. Siddiqi, R. Simmonds, M. Singh, I. Spielman, K. Temme, D. S. Weiss, J. Vučković, V. Vuletić, J. Ye, and M. Zwierlein, PRX Quantum **2**, 017003 (2021).

[36] S. Endo, Z. Cai, S. C. Benjamin, and X. Yuan, Journal of the Physical Society of Japan **90**, 032001 (2021), https://doi.org/10.7566/JPSJ.90.032001.

[37] M. Cerezo, A. Poremba, L. Cincio, and P. J. Coles, Quantum **4**, 248 (2020).

[38] K. Bharti, A. Cervera-Lierta, T. H. Kyaw, T. Haug, S. Alperin-Lea, A. Anand, M. Degroote, H. Heimonen, J. S. Kottmann, T. Menke, W.-K. Mok, S. Sim, L.-C. Kwek, and A. Aspuru-Guzik, Rev. Mod. Phys. **94**, 015004 (2022).

[39] D. Cleland, G. H. Booth, and A. Alavi, The Journal of chemical physics **132**, 041103 (2010).

[40] A. Peruzzo, J. McClean, P. Shadbolt, M.-H. Yung, X.-Q. Zhou, P. J. Love, A. Aspuru-Guzik, and J. L. O?brien, Nature communications **5**, 1 (2014).

[41] H. R. Grimsley, S. E. Economou, E. Barnes, and N. J. Mayhall, Nature comm. **10**, 1 (2019).

[42] A. Abbas, D. Sutter, C. Zoufal, A. Lucchi, A. Figalli, and S. Woerner, Nature Computational Science **1**, 403 (2021).

[43] Z. Holmes, K. Sharma, M. Cerezo, and P. J. Coles, (2021), arXiv:2101.02138 [quant-ph].

[44] Y. Li and S. C. Benjamin, Phys. Rev. X **7**, 021050 (2017).

[45] K. Temme, S. Bravyi, and J. M. Gambetta, Phys. Rev. Lett. **119**, 180509 (2017).

[46] S. Endo, S. C. Benjamin, and Y. Li, Phys. Rev. X **8**, 031027 (2018).

[47] Y. Kim, C. J. Wood, T. J. Yoder, S. T. Merkel, J. M. Gambetta, K. Temme, and A. Kandala, "Scalable error mitigation for noisy quantum circuits produces competitive expectation values," (2021).

[48] M. Cerezo and P. J. Coles, arXiv e-prints , arXiv (2020).

[49] S. Wang, E. Fontana, M. Cerezo, K. Sharma, A. Sone, L. Cincio, and P. J. Coles, Nature Communications **12** (2021), 10.1038/s41467-021-27045-6.

[50] L. Bittel and M. Kliesch, Phys. Rev. Lett. **127**, 120502 (2021).

[51] M. Troyer and U.-J. Wiese, Physical review letters **94**, 170201 (2005).

[52] J. Klassen, M. Marvian, S. Piddock, M. Ioannou, I. Hen, and B. M. Terhal, SIAM Journal on Computing **49**, 1332 (2020), https://doi.org/10.1137/19M1287511.

[53] D. Hangleiter, I. Roth, D. Nagaj, and J. Eisert, Science advances **6**, eabb8341 (2020).

[54] G. Torlai, J. Carrasquilla, M. T. Fishman, R. G. Melko, and M. P. A. Fisher, Phys. Rev. Research **2**, 032060 (2020).

[55] R. Levy and B. K. Clark, Phys. Rev. Lett. **126**, 216401 (2021).

[56] K. M. Nakanishi, K. Mitarai, and K. Fujii, Phys. Rev. Research **1**, 033062 (2019).

[57] R. M. Parrish, E. G. Hohenstein, P. L. McMahon, and T. J. Martínez, Phys. Rev. Lett. **122**, 230401 (2019).

[58] Z.-J. Zhang, T. H. Kyaw, J. Kottmann, M. Degroote, and A. Aspuru-Guzik, Quantum Science and Technology (2021).

[59] H. L. Tang, V. Shkolnikov, G. S. Barron, H. R. Grimsley, N. J. Mayhall, E. Barnes, and S. E. Economou, arXiv preprint arXiv:1911.10205 (2019).

[60] H. L. Tang, V. Shkolnikov, G. S. Barron, H. R. Grimsley, N. J. Mayhall, E. Barnes, and S. E. Economou, PRX Quantum **2**, 020310 (2021).

[61] Y. Fan, C. Cao, X. Xu, Z. Li, D. Lv, and M.-H. Yung, arXiv preprint arXiv:2106.15210 (2021).

[62] Note that we can reuse the result of $|H_{ji}|$ and $H_{ji}/|H_{ji}|$, if we have already obtained them in previous steps.

[63] All the energy and standard deviation are evaluated by taking energies after reaching a certain total evolution time, and usually after the total number of walkers stabilizes.
[64] D. Wecker, M. B. Hastings, and M. Troyer, Physical Review A **92**, 042303 (2015).
[65] C. Cade, L. Mineh, A. Montanaro, and S. Stanisic, Physical Review B **102**, 235122 (2020).
[66] Z. Cai, Physical Review Applied **14**, 014059 (2020).
[67] Z.-X. Li and H. Yao, Annual Review of Condensed Matter Physics **10**, 337 (2019).
[68] W. J. Huggins, B. A. O'Gorman, N. C. Rubin, D. R. Reichman, R. Babbush, and J. Lee, Nature **603**, 416 (2022).
[69] X. Xu and Y. Li, arXiv e-prints , arXiv:2205.14903 (2022), arXiv:2205.14903 [quant-ph].
[70] G. Mazzola and G. Carleo, arXiv e-prints , arXiv:2205.09203 (2022), arXiv:2205.09203 [quant-ph].